A filamentary structure of massive star-forming galaxies associated with an X-ray absorbed QSO at z=1.8

J. A. Stevens

Astronomy Technology Centre, Royal Observatory, Blackford Hill, Edinburgh EH9 3HJ, UK

`jas@roe.ac.uk`

M. J. Page

Mullard Space Science Laboratory, University College London, Holmbury St. Mary, Dorking, Surrey RH5 6NT, UK

`mjp@mssl.ucl.ac.uk`

R. J. Ivison

Astronomy Technology Centre, Royal Observatory, Blackford Hill, Edinburgh EH9 3HJ, UK

`rji@roe.ac.uk`

Ian Smail

Institute for Computational Cosmology, University of Durham, South Road, Durham DH1 3LE

`ian.smail@durham.ac.uk`

and

F. J. Carrera

Instituto de Fisica de Cantabria (Consejo Superior de Investigaciones Cientificas-Universidad de Cantabria), Avenida de los Castros 39005 Santander, Spain

`carreraf@ifca.unican.es`

ABSTRACT

The genesis of spheroids is central to our understanding of galaxy formation – they are relatively simple systems, containing about half the stellar mass of the Universe. A major subset of spheroids, massive elliptical galaxies, are preferentially found in clusters where they exhibit old, coeval stellar populations suggesting that they formed synchronously at early epochs. Here we report SCUBA submillimeter imaging of a region around a $z = 1.8$ X-ray selected QSO. The image reveals a remarkable ~ 400 kiloparsec long chain of galaxies each with an obscured star-formation rate sufficiently high to build a massive spheroid in less than 1 Gyr. The large over-density of these galaxies relative to expectations for a random field implies they probably reside in a structure associated with the QSO. We suggest that this star formation is associated with galaxy mergers or encounters within the filament, such as those predicted by the popular hierarchical model of galaxy formation. Our observations suggest that strong absorption in the X-ray spectra of QSOs at high-redshifts may result from a veil of gas thrown up by a merger or merger-induced activity, rather than an orientation-dependent obscuring torus. It is argued that these systems are the precursors of elliptical galaxies found today in the core regions of all rich galaxy clusters.

Subject headings: galaxies: evolution – galaxies: formation

1. Introduction

Hierarchical structure formation models are predicated on the assumption that structures grow via the gravitational collapse of small inhomogeneities in a Gaussian random field. Within such a model it is expected that galaxies and larger scale structures will form at local maxima of the density field (Kaiser 1984). Inhomogeneities in such over-dense regions, that will go on to become the most massive rich clusters at the present day, tend to collapse earlier than similar inhomogeneities in less-dense regions (Kauffmann 1996). Moreover, although the power spectrum of the fluctuations in these models are scale free, detailed numerical simulations show that they naturally create large-scale filamentary structures with the most massive bound systems, such as rich clusters, forming at intersections and junctions of these filaments (Colberg et al. 1999). There is expected to be considerable cross-talk between structures forming on different scales in these models: with galaxy halos growing through major mergers within the larger-scale filaments and streaming down these into the forming cluster. These galaxies are most naturally identified as the progenitors of the homogeneous population of old, luminous elliptical galaxies which reside in rich clusters at the present day. These models thus predict that the forming elliptical galaxies should be distributed in a highly anisotropic fashion around the collapsing protocluster (West 1984).

To test these predictions requires observations in a waveband sensitive to massive star formation at high redshifts. Recent progress in submillimeter astronomy has shown that star formation in massive galaxies at high redshifts is not a luminous phenomenon at optical wavelengths because of the obscuring effect of dust (Smail et al. 2002). The reprocessed starlight peaks at far-infrared wavelengths in the rest frame of the source and is shifted into the submillimeter waveband at $z > 1$. We also require a method of identifying an over-dense region of the early Universe. One method is to target powerful active galactic nuclei (AGN). Submillimeter images of the ~ 1 Mpc-scale fields around such AGN (high-redshift radio galaxies – HzRGs) at $z > 3$ show extended dust emission associated with the AGN, and luminous submillimeter companions (Ivison et al. 2000; Stevens et al. 2003), several of which are confirmed to be at the same redshifts as the radio galaxies (Smail et al. 2003a,b). While these results provide support for models of biased galaxy formation, they relate only to a very rare class of tracer galaxies, powerful HzRGs at $z > 3$. Therefore, if we are to investigate the formation of structures the size of typical clusters then less extreme, lower mass signpost AGN at lower redshifts must be identified and their environments mapped at submillimeter wavelengths. With these points in mind we have initiated a programme to image the fields around $1.5 < z < 3$ QSOs detected in the submillimeter waveband (Page et al. 2001). Here we report the first submillimeter imaging observations of one of these QSOs, RXJ094144.51+385434.8 at $z = 1.819$.

A Hubble constant $H_0 = 70\ \mathrm{km\,s^{-1}\,Mpc^{-1}}$ and density parameters $\Omega_\Lambda = 0.7$ and $\Omega_\mathrm{m} = 0.3$ are assumed throughout this Letter.

2. Observations and data reduction

2.1. Submillimeter imaging

Observations were made with SCUBA (Holland et al. 1999) at the JCMT in 2003 February and March. During all three nights on which data were gathered, weather conditions were in the top quartile of those experienced on Mauna Kea. We used 'jiggle-map' mode to make simultaneous maps at 450 and 850 μm. The secondary mirror was chopped $45''$ in right ascension, and the antenna was nodded every 16 seconds. The resulting maps thus show the negative off-positions of real sources (they have not been 'cleaned'). The atmospheric opacity was monitored with regular skydips, and flux density calibration was made on each night with jiggle-map observations of the standard source CRL618.

Data were analysed with the STARLINK package, SURF. Data were first corrected for beam-switching, flat-fielded and extinction corrected. We then removed residual sky emission and clipped each bolometer at the 5-σ level before resampling the data onto a RA/Dec grid and despiking at the 3-σ level. Pointing drifts were corrected for with linear interpolation between the measured offsets (in all cases less than $2''$). After flux density calibration, the data were rebinned to make the final signal and noise maps. For this process we used an adapted version of the SURF task, REBIN – the standard deviation of the signal for each bolometer in each observation was first calculated, the data were then rebinned onto a $1''$ grid in RA/Dec coordinates, and the standard deviations were used to create weighted signal and weighted noise maps. These maps were subsequently smoothed with a $6''$ (at 850 μm) or $4''$ (at 450 μm) Gaussian.

2.2. Optical and near-infrared imaging

An R-band image of a $16' \times 16'$ region centered on the QSO was taken at the 4.2-m William Herschel Telescope (WHT) using the Prime Focus Imaging Camera on the night of 2003 May 28. The total integration time was 3.7 ks, the seeing was $1.0''$ and the conditions were photometric. The data were reduced using standard IRAF scripts and calibrated using Landolt faint standards (Landolt 1992). The 5-σ limiting magnitude for a point-source in our $2.5''$ aperture is $R = 25.4$.

A K-band exposure of the central $90'' \times 90''$ part of the field was obtained in photometric conditions with the UFTI imager on the United Kingdom Infra-Red Telescope (UKIRT) on 2003 May 24. The total exposure time was 7.7 ks in $0.6''$ seeing yielding a 5-σ limiting magnitude of $K = 20.5$. The data were reduced using the ORAC-DR pipeline and the resulting mosaics combined with STARLINK CCDPACK tasks. The data were calibrated with observations of the UKIRT faint standard FS 127 (Hawarden et al. 2001).

Galaxies were identified on the K-band frame using SExtractor (Bertin & Arnouts 1996) and total magnitudes estimated from BEST_MAG. The positions were then used to measure colors within $2.5''$ diameter apertures from the seeing-matched R/K frames.

3. Results and Discussion

The 450- and 850-μm images reveal a remarkable structure of submillimeter sources in the field of the QSO, particularly striking at 450 μm (Fig. 1). For the high redshift ($z > 3$) objects targeted to date (Stevens et al. 2003), the slightly different negative K-corrections that act on the 850- and 450-μm flux densities have resulted in poor quality 450-μm images. This is because, while the 850-μm datum is shifted along the steep Rayleigh-Jeans tail of the dust emission, effectively canceling out the cosmological dimming, the 450-μm datum is shifted close to the peak of this emission giving a marked fall-off of the flux density with redshift. In this respect, the lower redshift of RXJ094144.51+385434.8 has worked to our advantage, providing us with an image of the submillimeter dust emission with unprecedented resolution ($8.5''$, equivalent to $\sim$70 kpc at $z = 1.8$).

We identify six sources with peak signal-noise greater than 3 in the 450-μm image; they trace a 'chain' of submillimeter galaxies with an extent of at least 400 kpc (if at $z = 1.8$). Source names, coordinates and physical quantities calculated from the images are presented in Table 1. At 450 μm the sources are well enough separated to allow good estimation of their individual flux densities; this is not the case at 850 μm where we give combined flux densities for Nos 1,2 (the QSO) and 4,5. Quoted errors do not include the calibration uncertainties which are about 10% at 850 μm and 15–20% at 450 μm. Dust masses are calculated from the 450 μm flux densities in the standard manner (Hildebrand 1983), adopting a value for the dust mass absorption coefficient $\kappa_{100\mu m} = 5.5\,\mathrm{m}^2\,\mathrm{kg}^{-1}$ (Draine & Lee 1984). Far-infrared luminosities (L_{FIR}) are calculated by scaling the 450 μm emission with that of Mrk 231 which has $L_{\mathrm{FIR}} = 2.0 \times 10^{12}\ L_{\odot}$ (calculated from a grey-body fit to the far-infrared–millimeter SED - the fitted dust temperature is 42 K). Using Arp220 as a template reduces the L_{FIR} estimates by a factor ~ 1.6. The star-formation rates are calculated from SFR($\mathrm{M}_{\odot}$/yr)= $L_{\mathrm{FIR}}/(5.8 \times 10^9 L_{\odot})$ (Kennicutt 1998).

Each galaxy in this filament is itself a very massive ultraluminous infrared galaxy (ULIRG) producing stars at a rate sufficient to build a massive spheroid in < 1 Gyr. Let us assess the significance of this structure. The density of 450-μm sources in this field is 1.4$\pm$0.6 arcmin^{-2}, disregarding the QSO which was already known to be a submillimeter source. The corresponding density of sources found in 'blank field' surveys with 450-μm flux densities in excess of 30 mJy is uncertain, but best estimates lie in the range $0.03 - 0.14$ arcmin^{-2} (Smail et al. 2002). These figures thus imply an order of magnitude over-density of luminous star-forming galaxies in the 3.5 arcmin^{-2} field around RXJ094144.51+385434.8. We can investigate the statistical significance of this over-density by calculating the combined probability that these sources each exist at a distance, d, from the QSO given the expectation from the known surface density of blank field objects. The high end of the range given above, i.e. $n = 0.14$ arcmin^{-2}, gives the most pessimistic estimate of this probability (given by $P = 1 - \exp\{-\pi n d^2\}$ for each source). We find $P = 2.9 \times 10^{-7}$ that the structure we observe is a chance superposition of field objects ($P = 6.5 \times 10^{-5}$ if source 2 is excluded). This result provides very strong evidence that the companion galaxies lie at the same redshift and in the same structure as the QSO. Assuming this to be true, the star formation rate density calculated in a 500 kpc cube centered on this structure is $> 1000\ \mathrm{M}_{\odot}\ \mathrm{yr}^{-1}\ \mathrm{Mpc}^{-3}$, about 3 to 4 orders of magnitude higher than found in unbiased optical, infrared and submillimeter surveys (Ivison et al. 2002; Chapman et al. 2003). This field thus provides a striking demonstration of the filamentary distribution of forming galaxies in a high-density region at high redshift.

Can we find further support for the hierarchical model in our data? In the high resolution 450-μm image, the central QSO and at least one of the spatially distinct submillimeter sources have complex morphologies, indicative of either merging or interacting systems. These characteristics are analogous to those observed in local ULIRGs (Joseph 1990) although these have more compact millimeter/submillimeter emission (Downes & Solomon 1998) than observed here at higher redshift. Moreover, these mergers must be occurring between similarly massive (Table 1) and gas rich systems, indicating that this activity is arising from major, rather than minor, mergers. Images of the RXJ094144.51+385434.8 field in the R- and K-band are shown in Fig. 2. The submillimeter galaxies RXJ094144SMM3, RXJ094144SMM4/5 and RXJ094144SMM6 all have counterparts identified as extremely red objects (EROs) (Elston, Rieke & Rieke 1988) – defined as having $(R - K) > 5.3$ (Pozzetti & Mannucci 2000). These objects are often found as counterparts to submillimeter galaxies discovered in blank field surveys (Smail et al. 1999; Ivison et al. 2002). The counterpart of RXJ094144SMM6 is particularly interesting; it has the appearance of an advanced merger and is a blue/red composite source, again similar to many counterparts of blank-field submillimeter galaxies (Ivison et al. 2002). Similar evidence for a merger origin of submillimeter galaxies has been seen in *Chandra* observations which show them to be coincident with two or three X-ray sources – interpreted as obscured AGN buried in merging star-forming galaxies (Smail et al. 2003a; Alexander 2004). If the submillimeter-detected galaxies are proto-ellipticals then at $z \sim 2$ they should contain growing black holes which shine as AGN (Kauffmann & Haehnelt 2000; Page et al. 2001). However, the *ROSAT* data for this field show that the QSO is the only luminous X-ray source amongst them. If the other dusty galaxies contain AGN then they have to be of lower luminosity or more highly obscured or both. Observations with the new generation of X-ray telescopes will allow us to probe the evolutionary state of the black holes in these systems (Smail et al. 2003a).

These images are the first to be made of a high redshift, X-ray absorbed QSO at submillimeter wavelengths. The importance of these objects relative to their better studied X-ray unabsorbed (or optically selected) counterparts is only just becoming clear. For matched $(1 < z < 3)$ samples selected close to the break of the X-ray luminosity function, the latter are about one order of magnitude less luminous at submillimeter wavelengths. The most likely interpretation is that the X-ray absorption in these objects is not linked with orientation dependent obscuration - the ‘unified scheme’ (Antonucci 1993) - but rather with the evolutionary state of the galaxy (Page et al. 2004). Our submillimeter images indicate that this is indeed the case for RXJ094144.51+385434.8 – its submillimeter luminosity appears to originate in large scale star formation associated with a major galaxy merger.

Finally, let us consider the fate of this structure. Deep *HST* images of the fields around QSOs (McLure & Dunlop 2001) suggest that their typical environments are galaxy clusters of Abell richness class 0 (Abell 1958). At the present day such clusters contain within their virial radius of order 10 galaxies with luminosity greater than or equal to L^* (Christlein & Zabludoff 2003). If the 6 submillimeter luminous galaxies in the protocluster around RXJ094144.51+385434.8 continue to form stars at the rates inferred from their submillimeter luminosities (Table 1) then their transformation into L^* ellipticals will be complete within in a fraction of a Gyr. We can thus conclude that the coeval stellar populations of the luminous cluster galaxies will be in place by redshift 1.7. Their subsequent passive luminosity evolution will naturally result in a population of ellipticals with properties that match the core regions of today's rich galaxy clusters.

The James Clerk Maxwell Telescope is operated by the Joint Astronomy Centre in Hilo, Hawaii on behalf of the parent organizations PPARC in the United Kingdom, the National Research Council of Canada and the Netherlands Organization for Scientific Research. Near-infrared data were collected as part of the UKIRT Service Programme. UKIRT is operated by the Joint Astronomy Centre on behalf of PPARC. The WHT is operated on the island of La Palma by the Isaac Newton Group in the Spanish Observatorio del Roque de los Muchachos of the Instituto de Astrofisica de Canarias. J.A.S. acknowledges support from PPARC, I.R.S. from the Royal Society and F.J.C. from the Spanish Ministerio de Cienca y Technología, under project AYA2000-1690.

REFERENCES

Abell, G. 1958, ApJS, 3, 211

Alexander, D. M., Bauer, F. E., Chapman, S. C., Smail, I., Blain, A. W., Brandt, W. N., & Ivison, R. J. 2004, Multiwavelength mapping of galaxy formation and evolution, ed. R. Bender, & A. Renzini, ESO Astrophysics Symposium (Springer-Verlag), in press

Antonucci, R. 1993 ARA&A, 31, 473

Bertin, E., & Arnouts, S. 1996, A&AS, 117, 393

Chapman, S. C., Blain, A. W., Smail, I., & Ivison R. J. 2003, Nature, 422, 695

Christlein, D., & Zabludoff, A. I. 2003, ApJ, 591, 764

Colberg, J.M., White, S.D.M., Jenkins, A., & Pearce, F.R. 1999, MNRAS, 308, 593

Downes, D., & Solomon, P. M. 1998, ApJ, 507, 615

Draine, B. T., & Lee, H. M. 1984, ApJ, 285, 89

Elston, R., Rieke, G. H., & Rieke, M. J. 1988, ApJ, 331, 77

Hawarden T. G., Leggett, S. K., Letawsky M. B., Ballantyne D. R., & Casali, M. M. 2001, MNRAS, 325, 563

Hildebrand, R. D. 1983, QJRAS, 24, 267

Holland, W. S, et al. 1999, MNRAS, 303, 659

Ivison, R. J., et al. 2000, ApJ, 542, 27

Ivison, R. J., et al. 2002, MNRAS, 337, 1

Joseph, R. D. 1990, Dynamics and Interactions of Galaxies, ed. R. Wielen, Springer (New York), 132

Kaiser, N. 1984, ApJ, 284, L9

Kauffmann, G. 1996, MNRAS, 281, 487

Kauffmann, G., & Haehnelt, M. 2000, MNRAS, 311, 576

Kennicutt, R. C. 1998, ApJ, 498, 541

Landolt, A. U. 1992, AJ, 104, 340

McLure, R. J., & Dunlop, J. S. 2001, MNRAS, 321, 515

Page, M. J., Stevens, J. A., Mittaz, J. P. D., & Carrera, F. J. 2001, Science, 294, 2516

Page, M. J., Stevens, J. A., Ivison, R. J., & Carrera, F. J. 2004, Nature, submitted

Pozzetti, L., & Mannucci, F. 2000, MNRAS, 317, L17

Smail, I., et al. 1999, MNRAS, 308, 1061

Smail, I., Ivison, R. J., Blain, A. W., & Kneib, J.-P. 2002, MNRAS, 331, 495

Smail, I., Scharf, C. A., Ivison, R. J., Stevens, J. A., Bower, R. G., & Dunlop, J. S. 2003a, ApJ, 599, 86

Smail, I., Ivison, R. J., Gilbank, D. G., Dunlop, J. S., Keel, W. C., Motohara, K. & Stevens, J. A. 2003b, ApJ, 583, 551

Stevens J. A., et al. 2003a, Nature, 425, 264

West, M. J. 1984, MNRAS, 268, 79

Table 1. Source names, coordinates, submillimeter flux densities and parameters.

No.[a]	Source name[b]	RA (J2000.0)[c]	Dec (J2000.0)[c]	S_{850}(mJy)	S_{450}(mJy)	Dust Mass ($M_\odot$)	$L_{\rm FIR}(L_\odot)$	SFR($M_\odot$/yr)
1	RXJ094144SMM1	09 41 44.96	+38 54 39.0	13.4 ± 1.5[d]	44.3 ± 7.6	7.1×10^8	1.6×10^{13}	2700
2	RXJ094144SMM2	09 41 44.49	+38 54 42.0		29.8 ± 7.9	4.8×10^8	1.1×10^{13}	1800
3	RXJ094144SMM3	09 41 44.00	+38 54 24.8	6.6 ± 1.5	32.6 ± 8.3	5.3×10^8	1.1×10^{13}	2000
4	RXJ094144SMM4	09 41 46.63	+38 54 15.8	8.0 ± 1.3	33.3 ± 8.9	5.4×10^8	1.2×10^{13}	2000
5	RXJ094144SMM5	09 41 46.16	+38 54 16.0		37.8 ± 9.4	6.1×10^8	1.3×10^{13}	2300
6	RXJ094144SMM6	09 41 46.48	+38 53 58.8	6.5 ± 1.8	39.7 ± 8.6	6.4×10^8	1.4×10^{13}	2400

[a] Source Nos are those printed on Fig. 1.

[b] Source names are based on the *ROSAT* right ascension position of the QSO.

[c] Source coordinates are taken from the 450-μm map which is centred on the QSO at $09^{\rm h}41^{\rm m}44^{\rm s}.51$, $+38^\circ 54' 34''.8$ (J2000.0). The formal uncertainties on these positions, given by FWHM/(S/N×2) are only $0.7 - 1.2''$ although it should be assumed that systematic effects will at least double these values.

[d] The QSO - cf. 10.1 ± 1.7 mJy from Page et al. (2001)

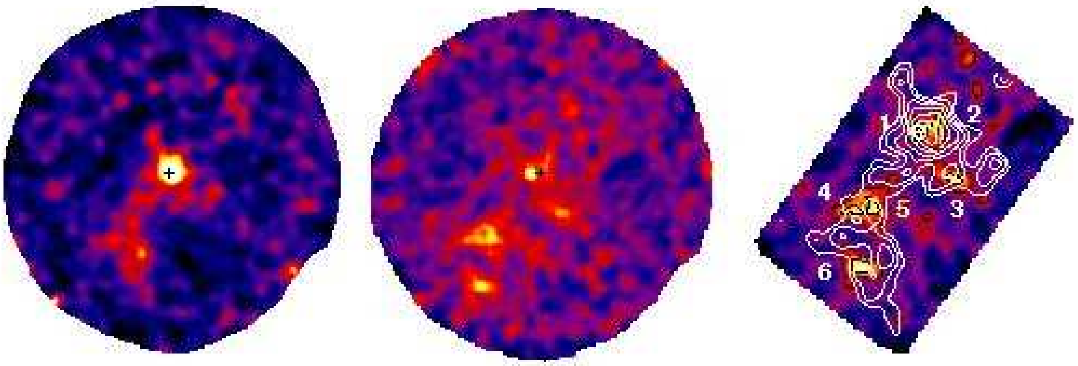

Fig. 1.— Submillimeter imaging of the field around RXJ094144.51+385434.8. The left-hand panel shows the SCUBA 850-μm image (diameter $\sim 150''$, resolution $14.8''$). The middle panel shows the corresponding 450-μm image (diameter $\sim 120''$, resolution $8.5''$). The right-hand panel shows a signal-to-noise image ($1.5' \times 1.0'$) at 450 μm (greyscale with black contours at 2, 3, 4 and 5σ) overlayed with the 850-μm signal-to-noise contours at 2, 3, 4, 5, 6, 7 and 8σ. The extent of the contoured region is $\sim$ 400 kpc. Numbers on the right-hand panel identify 450 μm sources with peak signal-to-noise greater than 3 - they correspond to those listed in Table 1. The optical position of the QSO is marked with a cross on the left-hand and middle panels.

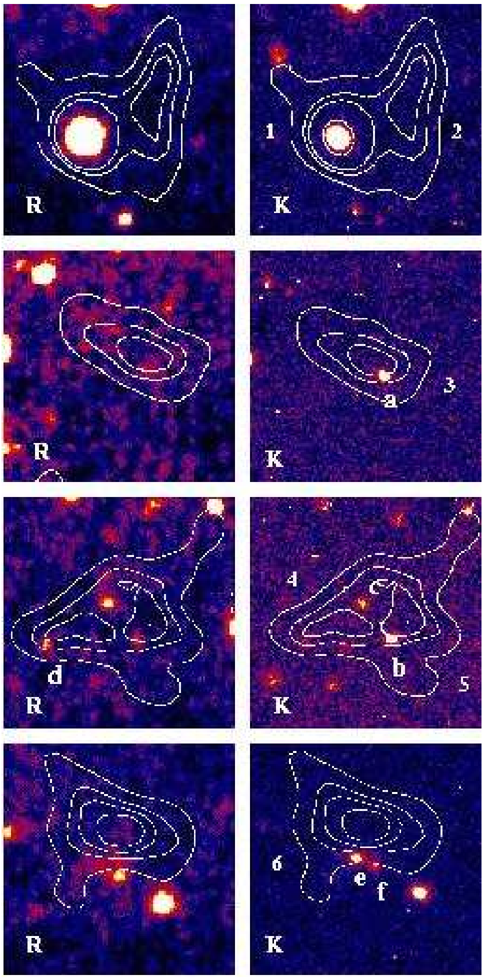

Fig. 2.— Optical and near-infrared imaging of the submillimeter galaxies in the vicinity of RXJ094144.51+385434.8. The RA/Dec images are 22″ square, equivalent to 200 kpc at $z = 1.8$. Optical R-band images (1″ seeing) from the WHT and near-infrared K-band images (0.6″ seeing) from UKIRT overlayed with the 450 μm contours from Fig. 1 (the 450 μm image has been offset by [−4.9″,+0.3″] to center the dust peak on the optical/near-infrared source). Numbers on the panels are those from Fig. 1 and Table 1. The magnitudes of these counterparts are (a) $K = 19.3$, $(R-K) = 5.8$ (b) $K = 19.9$, $(R-K) = 5.3$ (c) $K = 20.3$, $(R-K) = 3.9$ (d) $R = 24.9$, $(R-K) < 3.6$ (e) $K = 18.8$, $(R-K) = 5.4$ (f) $K = 19.5$, $(R-K) = 4.6$.